Hindawi
Advances in Civil Engineering
Volume 2021, Article ID 4767892, 17 pages
https://doi.org/10.1155/2021/4767892

*Research Article*

# Theoretical and Numerical Analysis of Soil-Pipe Pile Horizontal Vibration Based on the Fractional Derivative Viscoelastic Model

**Hao Zhang, Jienan Niu, Ningning Huang, and Qifang Yan**

*School of Architecture and Civil Engineering, Xinyang Normal University, Xinyang, Henan 464000, China*

Correspondence should be addressed to Hao Zhang; zhanghao@xynu.edu.cn

Received 27 August 2021; Accepted 27 October 2021; Published 18 November 2021

Academic Editor: Emanuele Brunesi



To describe the mechanical properties of the system of pipe pile-soil reasonably and accurately, the constitutive relations of the soil around pile and pile core soil are characterized by the fractional derivative viscoelastic model. We assume that the radial and circumferential displacements of the soil around the pile and pile core soil are the functions of $r$, $\theta$, and $z$. The horizontal dynamic control equations of soil layers are derived by using the fractional derivative viscoelastic model. Considering the fractional derivative properties, soil layer boundary condition, and contact condition of pile and soil, the potential function decomposition method is used to solve the radial and circumferential displacements of the soil layer. Then, the force of unit thickness soil layer on the pipe pile and the impedance factor of the soil layer are obtained. The horizontal dynamic equations of pipe pile are established considering the effect of soil layers. The horizontal dynamic impedance and horizontal-swaying dynamic resistance at the pile top are obtained by combining the pipe pile-soil boundary conditions and the orthogonal operation of trigonometric function. Numerical solutions are used to analyze the influence of pile and soil parameters on the soil impedance factor and horizontal dynamic impedance at pile top. The results show that the horizontal impedance factors of the soil layer and horizontal dynamic impedance of pipe pile by using the fractional derivative viscoelastic model can be degraded to those of the classical viscoelastic model and the elastic model. For the fractional derivative viscoelastic model of soil layer, the influence of soil around pile on the dynamic impedance is greater than that of pile core soil. The model parameter $T_{Oa}$, the inner radius of pipe pile, and the pile length have obvious effects on the horizontal impedance of the soil layer and pipe pile, while the influence of the pile core soil on the pile impedance is smaller.

## 1. Introduction

As a new viscoelastic constitutive model, the fractional derivative viscoelastic model has many advantages. For example, the model parameters can be determined by through inversion based on experiment data, numerical calculation, and software fitting. The model can describe the mechanical properties of materials under a relatively wide range of frequencies. Moreover, the model can not only well reflect the process of nonlinear gradual change at primary stage but also present accurately at steady stage and accelerated stage under high stress [1]. As a result, the model has been used in many fields such as viscoelastic mechanics, wave propagation, turbulence, control, stochastic diffusion, biomaterials, random wandering, and molecular spectroscopy [2–7]. Soil is a viscoelastic medium, but the application of fractional derivative viscoelastic models to the geotechnical engineering has only just started.

In recent years, more and more scholars employ the fractional derivative viscoelastic models to study the soil creep, consolidation, and vibration. On the basis of creep tests, Zhu et al. [8] proposed a fractional Kelvin–Voigt model to account for the time-dependent behavior of soil foundation under vertical line load based on the theory of viscoelasticity and fractional calculus and derived an analytical solution of settlements in the foundation using Laplace transforms; the results indicated that the settlement-time relationship can be accurately captured by varying the fractional orders of differential operator and the viscosity coefficients. Yin et al. [9] used a fractional derivative viscoelastic model to derive the stress-strain relationships of the

geomaterials under the condition of triaxial test. Based on the Nishihara model, Li et al. [10] established a fractional derivative-based creep model by the triaxial creep and shear tests of deep artificial frozen soil under different confining pressures and temperatures. Xu and Cui [11] proposed a fractional derivative creep model to describe the time-varying properties of Shanghai clay.

The pile-soil system is an important foundation form, which is widely used in civil and geotechnical engineering. Studying the dynamic characteristics of pile foundations and providing the theoretical basis for the design, construction, and testing of pile foundations are important because the pile foundations are subject to various dynamic loads. Some research results have been obtained on the dynamic characteristics of solid-core piles and the dynamic interaction of pile-soil [12–18]. With the development and application of pipe pile technology, the research on the dynamic characteristics of pipe pile has attracted sufficient attention. Liu et al. [19] studied the influence of soil plug effect on the dynamic response of large-diameter pipe piles during low-strain integrity testing and derived an analytical solution that can consider the stress wave propagating both in the vertical and circumferential directions in the frequency domain using the transfer function method. Cui et al. [20] proposed a new mechanical model for predicting the longitudinal vibration of pipe piles in the layered viscoelastic foundations, a dielectric viscous damping in the radial nonuniformity media was proposed by extending Novak's plane strain model and the complex stiffness method, and the analytical solutions for the system dynamic impedance, velocity conductance, and reflected signals were also obtained. Wu et al.[21] established the motion equations of the soil-pile system in the conditions of small deformation by considering the effect of soil plugging and additional mass and obtained the frequency-domain analytical solution of the vertical dynamic response of the pipe pile using the Laplace transform and the transfer function technique. A new method for the dynamic interaction between large-diameter floating pipe piles and the surrounding soil was proposed by Meng et al. [22], and the corresponding analytical solution of longitudinal complex impedance was obtained.

For the mechanical characteristics of pipe pile-soil system, most studies treated the soil layers as an elastic medium or a viscoelastic medium to derive the constitutive relationships of the soil layers; however, the classical elastic and viscoelastic methods have certain defects in describing the soil material properties. To more reasonably describe the constitutive relationships of the pile-soil system and investigate the mechanical properties of the pile-soil system under the dynamic load, this paper adopts the fractional derivative viscoelastic method to derive the horizontal dynamic control equations of pipe pile and soil layers. The potential function decomposition method is used to solve the radial and circumferential displacements of the pile-soil system. Moreover, the horizontal dynamic impedance and horizontal-swaying dynamic resistance at pile top are obtained by combining the pipe pile-soil boundary conditions and the orthogonal operation of trigonometric function. Finally, numerical solutions are used to analyze the influences of pile and soil parameters on the impedance factor of soil layers and the horizontal dynamic impedance of pipe pile.

## 2. Mathematical Models, Assumptions, and Control Equations

As shown in Figure 1, the end-bearing pipe pile in the soil vibrates horizontally under the horizontal dynamic load at the pile top.

The pipe pile is supported by the bedrock; the pipe pile length and the soil thickness are all $H$; the density and elastic modulus of the pipe pile are $\rho_{\mathrm{p}}$ and $E_{\mathrm{p}}$, respectively; the inner and outer radii of the pipe pile are $r_{\mathrm{O}}$ and $r_{\mathrm{I}}$, respectively. The assumptions of the pipe pile-soil system are as follows: (1) the pipe pile and soil layers exhibit small deformation; (2) the pile core is completely filled with soil; (3) the pipe pile is completely in contact with the soil and bedrock, without the relative slip and dislodgement at the contact surface; and (4) the pipe pile is regarded as the circular tube elements, and the soil is regarded as viscoelastic media.

Because the classical viscoelastic model has certain defects in the description of the mechanical behavior of soil materials, the fractional derivative viscoelastic model is used to describe the stress-strain relationships of soil around the pile and the pile core soil [23]:

$$\left[1+\tau_{\beta b}^{\alpha_\beta}\frac{d^{\alpha_\beta}}{dt^{\alpha_\beta}}\right]\sigma_\beta=\left[1+\tau_{\beta a}^{\alpha_\beta}\frac{d^{\alpha_\beta}}{dt^{\alpha_\beta}}\right]\left[\lambda_\beta\left(\varepsilon_\beta\bullet I\right)I+2G_\beta\varepsilon_\beta\right], \tag{1}$$

where $\beta=O$ and $\beta=I$ denote the viscoelastic soil around the pile and the pile core soil, respectively; $\sigma_\beta$ and $\varepsilon_\beta$ denote the stress tensor and strain tensor of viscoelastic soil, respectively; $I$ is the unit matrix; $\tau_{\beta a}$ and $\tau_{\beta b}$ are the model parameters of the fractional derivative viscoelastic model; and $\lambda_\beta$ and $G_\beta$ are the Lamé constants for viscoelastic soil; $\lambda_\beta=2\mu_\beta/1-2\mu_\beta G_\beta$, where $\mu_\beta$ is Poisson's ratio of soil. $D^{\alpha_\beta}=d^{\alpha_\beta}/dt^{\alpha_\beta}$ is the $\alpha_\beta$ $(0<\alpha_\beta<1)$-order of the Riemann–Liouville fractional derivative, where $\alpha_\beta$ is the order of the fractional derivative, and the$\alpha_\beta$-order Riemann–Liouville fractional derivative [24] is

$$D^{\alpha_\beta}[x(t)]=\frac{1}{\Gamma\left(1-\alpha_\beta\right)}\frac{d}{dt}\int_0^t\frac{x(\tau)}{(t-\tau)^{\alpha_\beta}}\mathrm{d}\tau, \tag{2}$$

where $\Gamma$ represents the gamma function.

For the microelement of viscoelastic soil layer, the horizontal dynamic equations of fractional derivative viscoelastic soil layer [25] are

$$\begin{cases}\dfrac{\partial\sigma_{\beta rr}}{\partial r}+\dfrac{1}{r}\dfrac{\partial\sigma_{\beta r\theta}}{\partial\theta}+\dfrac{\partial\sigma_{\beta rz}}{\partial z}+\dfrac{\sigma_{\beta rr}-\sigma_{\beta\theta\theta}}{r}=\rho_\beta\dfrac{\partial^2u_{\beta r}}{\partial t^2},\\[2ex] \dfrac{\partial\sigma_{\beta r\theta}}{\partial r}+\dfrac{1}{r}\dfrac{\partial\sigma_{\beta\theta\theta}}{\partial\theta}+\dfrac{\partial\sigma_{\beta\theta z}}{\partial z}+2\dfrac{\sigma_{\beta r\theta}}{r}=\rho_\beta\dfrac{\partial^2u_{\beta\theta}}{\partial t^2},\end{cases} \tag{3}$$

where $\sigma_{\beta rr}$, $\sigma_{\beta\theta\theta}$, $\sigma_{\beta rz}$, and $\sigma_{\beta\theta z}$ are the radial, circumferential, and shear stresses of the viscoelastic soil, respectively, and

$u_{\beta r}$ and $u_{\beta\theta}$ are the radial and circumferential displacements of the viscoelastic soil, respectively.

The strain-displacement relationship of viscoelastic soil is

$$\varepsilon_\beta = \frac{1}{2}\left(\mathrm{grad}u_\beta + \mathrm{grad}^T u_\beta\right). \tag{4}$$

Ignoring the vertical displacement of the soil around pile and the pile core soil, equation (3) can be expressed by

$$\left(1+\tau_{\beta b}^{\alpha_\beta}\frac{d^{\alpha_\beta}}{dt^{\alpha_\beta}}\right)\left[\left(\lambda_\beta+2G_\beta\right)\frac{\partial\Delta_\beta}{\partial r}-\frac{2}{r}G_\beta\frac{\partial\omega_{\beta z}}{\partial\theta}+G_\beta\frac{\partial^2 u_{\beta r}}{\partial z^2}\right]=\rho\left(1+\tau_{\beta a}^{\alpha_\beta}\frac{d^{\alpha_\beta}}{dt^{\alpha_\beta}}\right)\frac{\partial^2 u_{\beta r}}{\partial t^2}, \tag{5}$$

$$\left(1+\tau_{\beta b}^{\alpha_\beta}\frac{d^{\alpha_\beta}}{dt^{\alpha_\beta}}\right)\left[\left(\lambda_\beta+2G_\beta\right)\frac{\partial\Delta_\beta}{r\,\partial\theta}+2G_\beta\frac{\partial\omega_{\beta z}}{\partial r}+G_\beta\frac{\partial^2 u_{\beta\theta}}{\partial z^2}\right]=\rho_\beta\left(1+\tau_{\beta a}^{\alpha_\beta}\frac{d^{\alpha_\beta}}{dt^{\alpha_\beta}}\right)\frac{\partial^2 u_{\beta\theta}}{\partial t^2}, \tag{6}$$

where $\Delta_\beta = 1/r\partial/\partial r\,(ru_{\beta r}) + 1/r\partial u_{\beta\theta}/\partial\theta$, $\omega_{\beta z} = 1/2r\,[\partial/\partial r\,(ru_{\beta\theta}) - \partial u_{\beta r}/\partial\theta]$, and $\rho_\beta$ is the soil density.

## 3. Horizontal Dynamic Solutions of Soil Layers Based on Fractional Derivative Viscoelastic Model

Since the pipe pile-viscoelastic soil system undergoes a steady-state vibration under the horizontal harmonic load of the pipe pile top, the radial and circumferential displacements of the soil around the pile, respectively, satisfy $u_{Or} = \widetilde{u}_{Or}e^{i\omega t}$ and $u_{O\theta} = \widetilde{u}_{O\theta}e^{i\omega t}$, where $\widetilde{u}_{\mathrm{Or}}$ and $\widetilde{u}_{O\theta}$ are the radial and circumferential dynamic amplitudes of the soil around the pile. The radial and circumferential displacements of the pile core soil satisfy $u_{Ir} = \widetilde{u}_{Ir}e^{i\omega t}$ and $u_{I\theta} = \widetilde{u}_{I\theta}e^{i\omega t}$, where $\widetilde{u}_{Ir}$ and $\widetilde{u}_{I\theta}$ are the dynamic amplitudes of the pile core soil. Substituting $u_{Or} = \widetilde{u}_{Or}e^{i\omega t}$, $u_{O\theta} = \widetilde{u}_{O\theta}e^{i\omega t}$, $u_{Ir} = \widetilde{u}_{Ir}e^{i\omega t}$, and $u_{I\theta} = \widetilde{u}_{I\theta}e^{i\omega t}$ into equations (5) and (6), respectively, considering the properties of fractional derivative, and reducing $e^{i\omega t}$ at both ends of the equation, the horizontal dynamic control equations of soil around the pile and the pile core soil can be expressed as

$$\left[1+\tau_{\beta b}^{\alpha_\beta}(i\omega)^{\alpha_\beta}\right]\left[\left(\lambda_\beta+2G_\beta\right)\frac{\partial\widetilde{\Delta}_\beta}{\partial r}-\frac{2}{r}G_\beta\frac{\partial\widetilde{\omega}_{\beta z}}{\partial\theta}+G_\beta\frac{\partial^2\widetilde{u}_{\beta r}}{\partial z^2}\right]=-\rho_\beta\omega^2\left[1+\tau_{\beta a}^{\alpha_\beta}(i\omega)^{\alpha_\beta}\right]\widetilde{u}_{\beta r}, \tag{7}$$

$$\left[1+\tau_{\beta b}^{\alpha_\beta}(i\omega)^{\alpha_\beta}\right]\left[\left(\lambda_\beta+2G_\beta\right)\frac{\partial\widetilde{\Delta}_\beta}{r\,\partial\theta}+2G_\beta\frac{\partial\widetilde{\omega}_{\beta z}}{\partial r}+G_\beta\frac{\partial^2\widetilde{u}_{\beta\theta}}{\partial z^2}\right]=-\rho_\beta\omega^2\left[1+\tau_{\beta a}^{\alpha_\beta}(i\omega)^{\alpha_\beta}\right]\widetilde{u}_{\beta\theta}, \tag{8}$$

where $T_{Oa} = \tau_{Oa}v_O/H$, $\widetilde{\omega}_{\beta z} = 1/2r\,[\partial/\partial r\,(r\widetilde{u}_{\beta\theta}) - \partial\widetilde{u}_{\beta r}/\partial\theta]$, and $\beta = O$ and $\beta = I$ denote the viscoelastic soil around the pile and the pile core soil, respectively.

As, $\overline{r} = r/H$, $\overline{z} = r/H$, $\overline{\omega} = H\omega/v_O$, $\overline{u}_{\beta r} = \widetilde{u}_{\beta r}/H$, $\overline{u}_{\beta\theta} = \widetilde{u}_{\beta\theta}/H$, $v_O = \sqrt{G_O/\rho_O}$, $T_{Oa} = \tau_{Oa}v_O/H$, $T_{Ob} = \tau_{Ob}\ v_O/H$, $\tau_1 = \tau_{Ia}/\tau_{Oa}$, $\tau_2 = \tau_{Ia}/\tau_{Oa}$, $G = G_I/G_O$, $\rho = \rho_I/\rho_O$, equations (7) and (8) are dimensionless as follows:

$$\frac{2-2\mu_\beta}{1-2\mu_\beta}\frac{\partial\overline{\Delta}_\beta}{\partial\overline{r}}-\frac{2}{\overline{r}}\frac{\partial\overline{\omega}_{\beta z}}{\partial\theta}+\frac{\partial^2\overline{u}_{\beta r}}{\partial\overline{z}^2}=-\overline{\omega}^2\kappa_\beta^2\overline{u}_{\beta r}, \tag{9}$$

$$\frac{2-2\mu_\beta}{1-2\mu_\beta}\frac{\partial\overline{\Delta}_\beta}{\overline{r}\partial\theta}+2\frac{\partial\overline{\omega}_{\beta z}}{\partial\overline{r}}+\frac{\partial^2\overline{u}_{\beta\theta}}{\partial\overline{z}^2}=-\overline{\omega}^2\kappa_\beta^2\overline{u}_{\beta\theta}, \tag{10}$$

where $\kappa_O^2 = 1+T_{Oa}^{\alpha_O}(i\overline{\omega})^{\alpha_O}/1+T_{Ob}^{\alpha_O}(i\overline{\omega})^{\alpha_O}$, $\kappa_I^2 = 1+\tau_{Ia}^{\alpha_I}(i\omega)^{\alpha_I}/1+\tau_{Ib}^{\alpha_I}(i\omega)^{\alpha_I} = 1+(i\overline{\omega}\tau_1T_{Oa})^{\alpha_I}/1+(i\overline{\omega}\tau_2T_{Ob})^{\alpha_I}$, and $\nabla^2 = \partial^2/\partial\overline{r}^2 + 1/r\partial/\partial r + 1/r^2\partial^2/\partial\theta^2$.

By introducing the potential function,

$$\begin{aligned}
\overline{u}_{Or} &= \frac{\partial\phi_O}{\partial\overline{r}}+\frac{1}{\overline{r}}\frac{\partial\psi_O}{\partial\theta},\\
\overline{u}_{O\theta} &= \frac{1}{\overline{r}}\frac{\partial\phi_O}{\partial\theta}-\frac{\partial\psi_O}{\partial\overline{r}},\\
\overline{u}_{Ir} &= \frac{\partial\phi_I}{\partial\overline{r}}+\frac{1}{\overline{r}}\frac{\partial\psi_I}{\partial\theta},\\
\overline{u}_{I\theta} &= \frac{1}{\overline{r}}\frac{\partial\phi_I}{\partial\theta}-\frac{\partial\psi_I}{\partial\overline{r}}.
\end{aligned} \tag{11}$$

Decoupling equations (9) and (10),

$$\left(\nabla^2+\chi_\beta^2\frac{\partial^2}{\partial\overline{z}^2}+\zeta_\beta^2\right)\phi_\beta=0, \tag{12}$$

$$\left(\nabla^2+\frac{\partial^2}{\partial\overline{z}^2}+\eta_\beta^2\right)\psi_\beta=0, \tag{13}$$

where $\zeta_O^2 = \chi_O^2\overline{\omega}^2\kappa_O^2$, $\eta_O^2 = \overline{\omega}^2\kappa_O^2$, $\zeta_I^2 = \rho\overline{\omega}^2/G\chi_I^2\kappa_I^2$, $\eta_I^2 = \rho\overline{\omega}^2/G\kappa_I^2\zeta_I^2$, and $\chi_\beta = \sqrt{1-2\mu_\beta/2-2\mu_\beta}$.

The displacement of the soil at infinity is zero (when $r \longrightarrow \infty$, $u_{Or} \longrightarrow 0$, $u_{O\theta} \longrightarrow 0$), and the stress at surface of soil around the pile and the pile core soil is zero (when $z = H$, $\sigma_{Orz} = 0$, $\sigma_{O\theta z} = 0$, $\sigma_{Irz} = 0$, $\sigma_{I\theta z} = 0$). Considering the parity of the radial and circular displacements of soil, the boundedness of the pile core soil displacement, and the properties of the Bessel function, equations (12) and (13) can be solved using the separation of variables method. The series solutions of the potential function are

$$\phi_O = \cos\theta \sum_{k=1}^{\infty} A_{Ok} K_1(q_{Ok}\overline{r}) \sin(\alpha_{Ok}\overline{z}), \tag{14}$$

$$\psi_O = \sin\theta \sum_{k=1}^{\infty} B_{Ok} K_1(g_{Ok}\overline{r}) \sin(\alpha_{Ok}\overline{z}), \tag{15}$$

$$\varphi_I = \cos\theta \sum_{k=1}^{\infty} C_{Ik} I_1(q_{Ik}\overline{r}) \sin(\alpha_{Ik}\overline{z}), \tag{16}$$

$$\psi_I = \sin\theta \sum_{k=1}^{\infty} D_{Ik} K_1(g_{Ik}\overline{r}) \sin(\alpha_{Ik}\overline{z}), \tag{17}$$

where $q_O^2 = \alpha_{Ok}^2\chi_O^2 - \zeta_O^2$, $g_O^2 = \alpha_{Ok}^2 - \eta_O^2$, $q_I^2 = \alpha_{Ik}^2\chi_I^2 - \zeta_I^2$, $g_I^2 = \alpha_{Ik}^2 - \eta_I^2$, $\alpha_k = \alpha_{Ok} = \alpha_{Ik} = 2k - 1/2\pi$, $k = 1, 2, 3, \ldots \infty$; $A_{Ok}, B_{Ok}, C_{Ik}, D_{Ik}$ are the coefficients to be determined by the boundary conditions; and $I_1(\cdot)$ and $K_1(\cdot)$ are the first-order modified Bessel functions of type I and type II, respectively.

Considering equations (11) and (14)–(17), the series solutions of the radial and circumferential displacement of the soil layers are

$$\overline{u}_{Or} = \cos\theta \sum_{k=1}^{\infty} \left[ -\frac{A_{Ok}}{\overline{r}} K_1(q_{Ok}\overline{r}) - A_{Ok} q_{Ok} K_0(q_{Ok}\overline{r}) + \frac{B_{Ok} K_1(g_{Ok}\overline{r})}{\overline{r}} \right] \sin(\alpha_k \overline{z}), \tag{18}$$

$$\overline{u}_{O\theta} = \sin\theta \sum_{k=1}^{\infty} \left[ -\frac{A_{Ok} K_1(q_{Ok}\overline{r})}{\overline{r}} + \frac{B_{Ok}}{\overline{r}} K_1(g_{Ok}\overline{r}) + B_{Ok} g_{Ok} K_0(g_{Ok}\overline{r}) \right] \sin(\alpha_k \overline{z}), \tag{19}$$

$$\overline{u}_{Ir} = \cos\theta \sum_{k=1}^{\infty} \left[ q_{Ik} I_0(q_{Ik}\overline{r}) C_{Ik} - \frac{1}{\overline{r}} I_1(q_{Ik}\overline{r}) C_{Ik} + \frac{1}{\overline{r}} I_1(g_{Ik}\overline{r}) D_{Ik} \right] \sin(\alpha_{Ik}\overline{z}), \tag{20}$$

$$\overline{u}_{I\theta} = \sin\theta \sum_{k=1}^{\infty} \left[ -\frac{1}{\overline{r}} I_1(q_{Ik}\overline{r}) C_{Ik} - g_{Ik} I_0(g_{Ik}\overline{r}) D_{Ik} + \frac{1}{\overline{r}} I_1(g_{Ik}\overline{r}) D_{Ik} \right] \sin(\alpha_k \overline{z}). \tag{21}$$

Since it is assumed that the pipe pile is in complete contact with soil, considering the coordination of the pile-soil system and the forms of soil displacements, the dimensionless horizontal displacement of the pipe pile satisfies

$$U_p(\overline{z}) = \sum_{k=1}^{\infty} U_{pk} \sin(\alpha_k \overline{z}), \tag{22}$$

where $U_{pk}$ is the model amplitude independent of $z$. Considering that the pile-soil displacement at the contact surface satisfies $\overline{u}_{Or.} = U_p$, when $\overline{r} = \overline{r}_O, \theta = 0$; $\overline{u}_{O\theta} = -U_p$, when $\overline{r} = \overline{r}_O, \theta = \pi/2$; $\overline{u}_{Ir.} = U_p$, when $\overline{r} = \overline{r}_I, \theta = 0$; and $\overline{u}_{I\theta} = -U_p$, when $\overline{r} = \overline{r}_I, \theta = \pi/2$. Then, equations (18)–(21) can be expressed by

$$\sum_{k=1}^{\infty} \left[ -\frac{A_{Ok}}{\overline{r}_O} K_1(q_{Ok}\overline{r}_O) - A_{Ok} q_{Ok} K_0(q_{Ok}\overline{r}_O) + \frac{B_{Ok} K_1(g_{Ok}\overline{r}_O)}{\overline{r}_O} \sin(\alpha_k \overline{z}) \right] = \sum_{k=1}^{\infty} U_{pk} \sin(\alpha_k \overline{z}), \tag{23}$$

$$\sum_{k=1}^{\infty} \left[ -\frac{A_{Ok} K_1(q_{Ok}\overline{r}_O)}{\overline{r}_O} + \frac{B_{Ok}}{\overline{r}_O} K_1(g_{Ok}\overline{r}_O) + B_{Ok} g_{Ok} K_0(g_{Ok}\overline{r}_O) \right] \sin(\alpha_k \overline{z}) = -\sum_{k=1}^{\infty} U_{pk} \sin(\alpha_k \overline{z}), \tag{24}$$

$$\sum_{k=1}^{\infty} \left[ q_{Ik} I_0(q_{Ik}\overline{r}_I) C_{Ik} - \frac{1}{\overline{r}_I} I_1(q_{Ik}\overline{r}_I) C_{Ik} + \frac{1}{\overline{r}_I} I_1(g_{Ik}\overline{r}_I) D_{Ik} \sin(\alpha_{Ik}\overline{z}) \right] = \sum_{k=1}^{\infty} U_{pk} \sin(\alpha_k \overline{z}), \tag{25}$$

$$\sum_{k=1}^{\infty} \left[ -\frac{1}{\overline{r}_I} I_1(q_{Ik}\overline{r}_I) C_{Ik} - g_{Ik} I_0(g_{Ik}\overline{r}_I) D_{Ik} + \frac{1}{\overline{r}_I} I_1(g_{Ik}\overline{r}_I) D_{Ik} \right] \sin(\alpha_k \overline{z}) = -\sum_{k=1}^{\infty} U_{pk} \sin(\alpha_k \overline{z}). \tag{26}$$

The coefficients can be determined by solving equations (23)–(26):

$$\begin{aligned} A_{Ok} &= a_{Ok}U_{pk}, \\ B_{Ok} &= b_{Ok}U_{pk}, \\ C_{Ik} &= c_{Ik}U_{pk}, \\ D_{Ik} &= d_{Ik}U_{pk}, \end{aligned} \tag{27}$$

where $a_{Ok} = -2K_1(g_{Ok}\overline{r}_O) + g_{Ok}r_OK_0(g_{Ok}\overline{r}_O)/e_{Ok}$, $b_{Ok} = -2K_1(q_{Ok}\overline{r}_O) + q_{Ok}r_OK_0(q_{Ok}\overline{r}_O)/e_{Ok}$, $c_{Ik} = [g_{Ik}\overline{r}_II_0(g_{Ik}\overline{r}_I) - 2I_1(g_{Ik}\overline{r}_I)]/f_{Ik}$, $d_{Ik} = [q_{Ik}\overline{r}_II_0(q_{Ik}\overline{r}_I) - 2I_1(q_{Ik}\overline{r}_I)]/f_{Ik}$, $e_{Ok} = q_{Ok}K_0(q_{Ok}\overline{r}_O)K_1(g_{Ok}\overline{r}_O) + g_{Ok}K_1(q_{Ok}\overline{r}_O)K_0(g_{Ok}\overline{r}_O) + q_{Ok}g_{Ok}r_OK_0(q_{Ok}\overline{r}_O)K_0(g_{Ok}\overline{r}_O)$, and $f_{Ik} = q_{Ik}g_{Ik}\overline{r}_II_0(q\overline{r}_I)I_0(g_{Ik}\overline{r}_I) - g_{Ik}I_1(q_{Ik}\overline{r}_I)I_0(g_{Ik}\overline{r}_I) - q_{Ik}I_1(g_{Ik}\overline{r}_I)I_0(q_{Ik}r\overline{r}_I)$.

Based on equations (18)–(21), the corresponding radial stress and shear stress of the soil layers can be derived, and the forces of per unit thickness soil around the pile and pile core soil on pipe pile can be derived by the forms of series solutions:

$$\begin{aligned} F_O &= \int_0^{2\pi} [-\overline{\sigma}_{Or}\cos\theta + \overline{\tau}_{Or\theta}\sin\theta]|_{\overline{r}=\overline{r}_O}\overline{r}_O d\theta, \\ &= \pi\overline{r}_O\kappa_O^2\sum_{k=1}^{\infty}\left[\frac{2-2\mu_O}{1-2\mu_O}q_{Ok}^2K_1(q_{Ok}\overline{r}_O)a_{Ok} - g_{Ok}^2K_1(g_{Ok}\overline{r}_O)b_{Ok}\right]U_{pk}\sin(\alpha_k\overline{z}), \\ F_I &= \int_0^{2\pi} [\sigma_{Ir}\cos\theta - \tau_{Ir\theta}\sin\theta]|_{\overline{r}=\overline{r}_I}\overline{r}_I d\theta = \pi\overline{r}_I\kappa_I^2 G\sum_{k=1}^{\infty}\left[\frac{2-2\mu_I}{1-2\mu_I}q_{Ik}^2I_1(q_{Ik}\overline{r}_I)c_{Ik} + g_{Ik}^2I_1(g\overline{r}_I)d_{Ik}\right]U_{pk}\sin(\alpha_k\overline{z}). \end{aligned} \tag{28}$$

The resultant force of the unit thickness soil on the pipe pile is

$$\overline{P}_x = \pi\sum_{k=1}^{\infty}h_kU_k\sin(\alpha_k\overline{z}), \tag{29}$$

$$\begin{aligned} h_k = {} & \overline{r}_O\kappa_O^2\left[\frac{2-2\mu_O}{1-2\mu_O}q_{Ok}^2K_1(q_{Ok}\overline{r}_O)a_{Ok} - g_{Ok}^2K_1(g_{Ok}\overline{r}_O)b_{Ok}\right] \\ & + \overline{r}_I\kappa_I^2 G\left[\frac{2-2\mu_I}{1-2\mu_I}q_{Ik}^2I_1(q_{Ik}\overline{r}_I)c_{Ik} + g_{Ik}^2I_1(g_{Ik}\overline{r}_I)d_{Ik}\right], \end{aligned} \tag{30}$$

where $h_k$ is the impedance factor of the soil layer [25] and the real part and imaginary part of $h_k$ are the horizontal stiffness factor and the horizontal damping factor of the soil layer, respectively.

In this section, the dynamic solutions of the pile around soil and pile core soil under the horizontal harmonic load are obtained by the fractional derivative viscoelastic model. For the soil layer under the harmonic load with different frequencies, the variations of horizontal stiffness factor and the horizontal damping factor can be analyzed and discussed by equation (30).

## 4. The Numerical Analysis of Horizontal Impedance Factor of Soil Layer

In equation (35), $r_O/H = 1/20$, $r_I/H = 0.5/20$, $\rho = 1.0$; $G = 0.5$, $\rho_p = 2.0$, $E = 1000$, $\mu_O = 0.3$, $\mu_I = 0.3$, $T_{Oa} = 10$, $T_{Oa} = 20$, $\tau_1 = 0.5$, $\tau_2 = 0.5$, $\alpha_O = 0.5$, and $\alpha_I = 0.5$. With the variation of dimensionless frequency $H\omega/vO_s$, the variations of soil layer impedance factor are shown in Figures 2–10. For the first-order impedance factor, as the frequency $H\omega/vO_s$ is smaller than 1.8, the pile-soil interaction due to the pile top excitation causes the soil vibration and wave propagation, while the wave reflection and propagation in the vertical direction of the soil cause the resonance. Therefore, the horizontal stiffness factor of the soil layer decreases sharply with the increase of frequency. Near the frequency $H\omega/vO_s = 1.8$, the impedance factor forms an obvious resonance point, while the horizontal damping factor is close to the level. As the frequency $H\omega/vO_s$ continually increases, the horizontal stiffness factor and damping factor both increase gradually. From Figure 2, the frequency at the resonance point increases with the increase of the order $k$. At low frequency, the horizontal stiffness factor shows more obvious balance with the decrease of frequency, and the horizontal section length of the damping factor is longer.

For the fractional derivative viscoelastic model, classical viscoelastic model, and elastic model of soil, the comparison curves of soil horizontal impedance factors are shown in Figure 3. The impedance factor curves of fractional derivative viscoelastic model can gradually degenerate to the classical viscoelastic model and elastic model, which verifies the correctness of the results. Furthermore, the horizontal impedance factor of the classical viscoelastic model is the smallest, the horizontal impedance factor of the elastic model is the largest, and the horizontal impedance factor of the fractional derivative model is in between.

For different orders of the fractional derivative viscoelastic model, the horizontal impedance factor curves of the soil around the pile and the pile core soil are shown in Figures 4 and 5. For different orders of fractional derivative, the influence on the horizontal impedance factor of soil around the pile is larger than that of the pile core soil. The order of fractional derivative has almost no influence on the horizontal damping factor of the pile core soil. As the order of fractional derivative is larger, the stiffness factor and

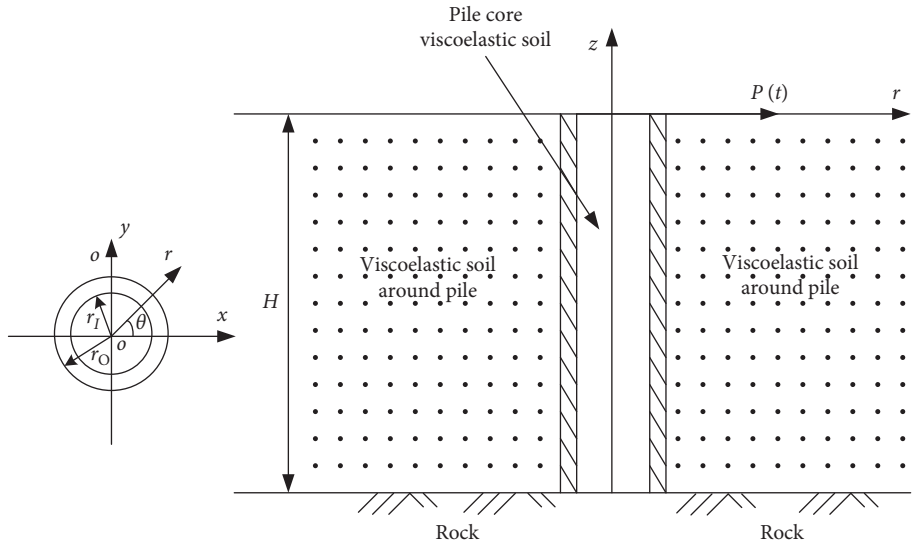


Figure 1: The model of soil layers and pipe pile.

damping factor of soil around the pile are smaller; however, the stiffness factor and damping factor of the pile core soil are larger.

As shown in Figure 6, the effects of the dimensionless model parameter $T_{Oa}$ on the horizontal stiffness factor and damping factor of soil around the pile are larger. As the parameter $T_{Oa}$ is larger, the stiffness factor and damping factor of soil around the pile are smaller. For the soil around pile and the pile core soil, the effects of model parameter ratios $\tau_1 = \tau_{Ia}/\tau_{Oa}$ and $\tau_2 = \tau_{Ib}/\tau_{Ob}$ on the horizontal impedance factor of soil layer are shown in Figures 7 and 8. The model parameters $\tau_1$ and $\tau_2$ have obvious effects on the horizontal stiffness factor of soil layer, while there are almost no effects on the horizontal damping factor. As the model parameter ratio $\tau_1$ is larger, the horizontal stiffness factor is smaller. However, the effects of model parameter ratio $\tau_2$ on the horizontal damping factor and stiffness factor are opposite.

The influences of the pipe-pile sizes on the impedance factor of soil layer are shown in Figures 9 and 10. As the inner radius of the pipe pile is larger, the wall thickness of the pipe pile is thinner, and the horizontal stiffness factor is smaller. The horizontal stiffness factor has a decreasing trend when the inner diameter is larger and the frequency is higher. However, the inner diameter has almost no influence on the horizontal damping factor. The influence of the pipe-pile length on the impedance factor of soil layer is larger. As the pipe pile is longer, the horizontal impedance factor is smaller.

## 5. Horizontal Dynamic Solution of Pipe Pile

To analyze the horizontal vibration of the pipe pile in soil layers based on the fractional derivative viscoelastic model, considering the dynamic equilibrium of pile microelement and the soil force of equation (29), the horizontal dynamic equation of pipe pile is

$$\frac{d^4 U_p(\overline{z})}{d\overline{z}} - \lambda^4 U_p(\overline{z}) = -\frac{4}{E\left(\overline{r}_O^4 - \overline{r}_I^4\right)} \sum_{k=1}^{\infty} h_k U_k \sin\left(\alpha_k \overline{z}\right), \tag{31}$$

where $\lambda^4 = 4\overline{\rho}_p \overline{\omega}^2 / E(\overline{r}_O^2 + \overline{r}_I^2)$, $\overline{\rho}_p = \rho_p/\rho_O$, and $E = E_p/G_O$.

The general solution of nonsingular equation (31) is

$$U_p = C_1 \cosh(\lambda\overline{z}) + C_2 \sinh(\lambda\overline{z}) + C_3 \cos(\lambda\overline{z}) + C_4 \sin(\lambda\overline{z}) - \frac{4}{E\left(\overline{r}_O^4 - \overline{r}_I^4\right)} \sum_{k=1}^{\infty} \frac{1}{\alpha_k^4 - \lambda^4} h_k U_k \sin\left(\alpha_k \overline{z}\right). \tag{32}$$

The coefficients can be obtained from the boundary conditions at the pile bottom and top.

Considering equations (22) and (32), the following relationship can be established:

$$C_1 \cosh(\lambda\overline{z}) + C_2 \sinh(\lambda\overline{z}) + C_3 \cos(\lambda\overline{z}) + C_4 \sin(\lambda\overline{z}) - \frac{4}{E\left(\overline{r}_O^4 - \overline{r}_I^4\right)} \sum_{k=1}^{\infty} \frac{1}{\alpha_k^4 - \lambda^4} h_k U_k \sin\left(\alpha_k \overline{z}\right) = \sum_{k=1}^{\infty} U_k \sin\left(\alpha_k \overline{z}\right). \tag{33}$$

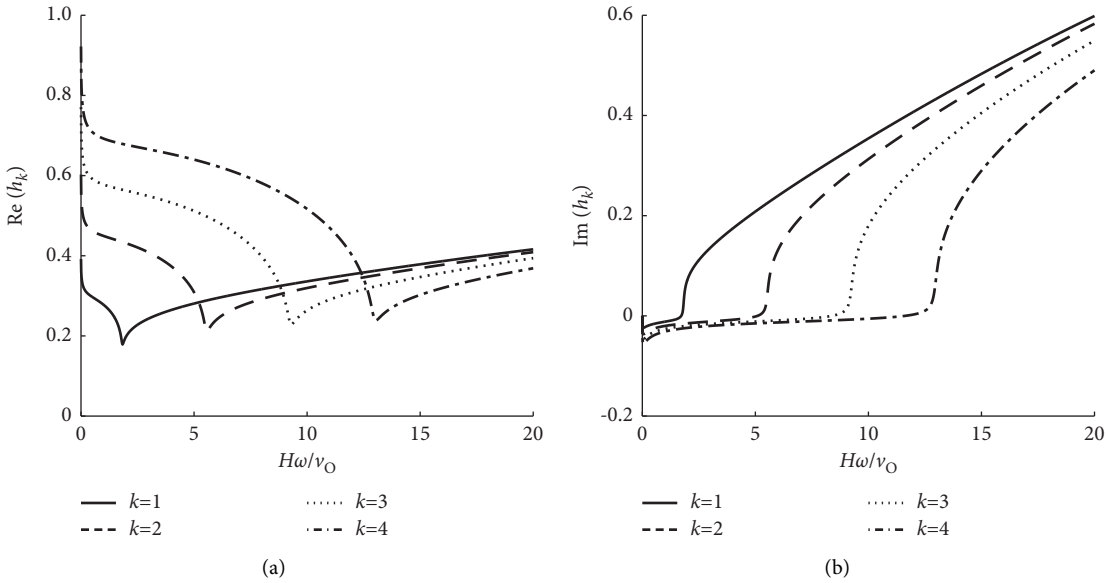


Figure 2: The impedance factor curves of the first to fourth order. (a) Horizontal stiffness factor of the soil layer. (b) Horizontal damping factor of the soil layer.

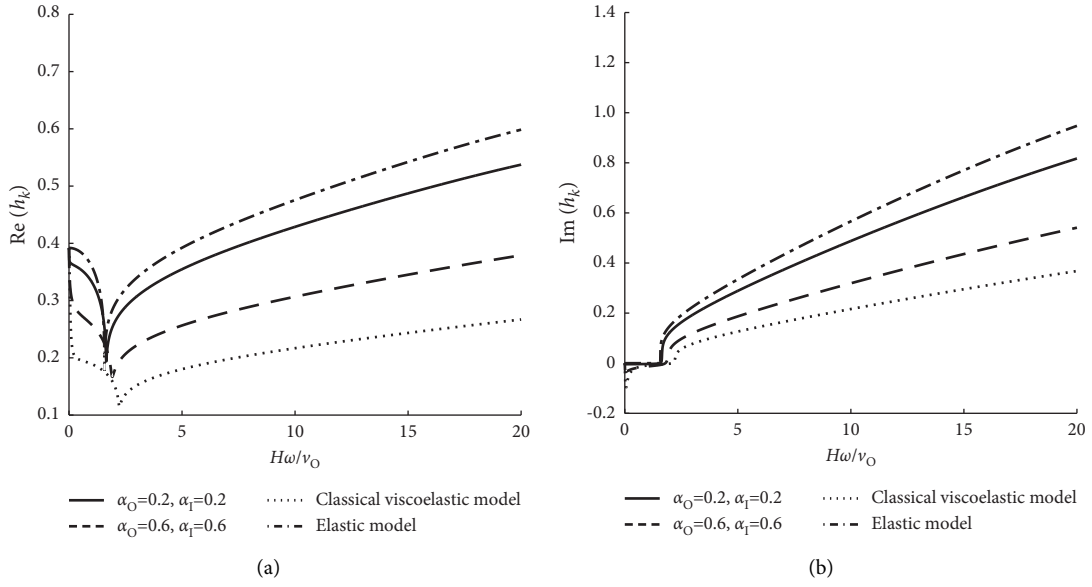


Figure 3: The first-order impedance factor curves of different soil models. (a) Horizontal stiffness factor of the soil layer. (b) Horizontal damping factor of the soil layer.

Using the orthogonality of trigonometric functions, equation (33) can be expressed as

$$U_k = \frac{2E\left(\overline{r}_O^4 - \overline{r}_I^4\right)\left(\alpha_k^4 - \lambda^4\right)}{E\left(\overline{r}_O^4 - \overline{r}_I^4\right)\left(\alpha_k^4 - \lambda^4\right) + 4h_k}\left(f_{1k}C_1 + f_{2k}C_2 + f_{3k}C_3 + f_{4k}C_4\right), \tag{34}$$

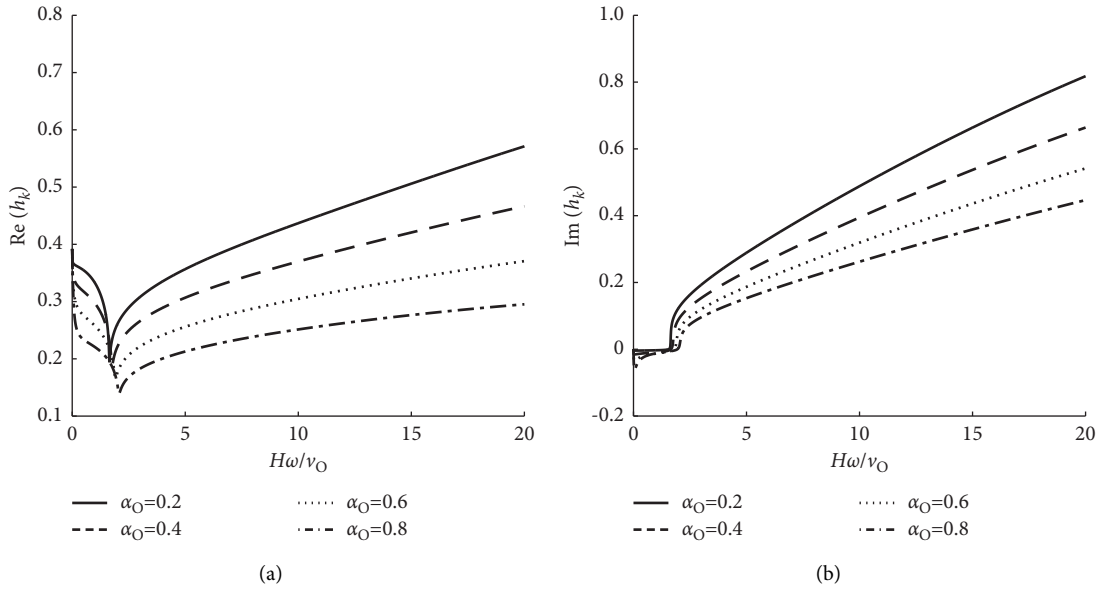


Figure 4: The impedance factor curves of pile around soil under different fractional derivative orders. (a) Horizontal stiffness factor of the soil layer. (b) Horizontal damping factor of the soil layer.

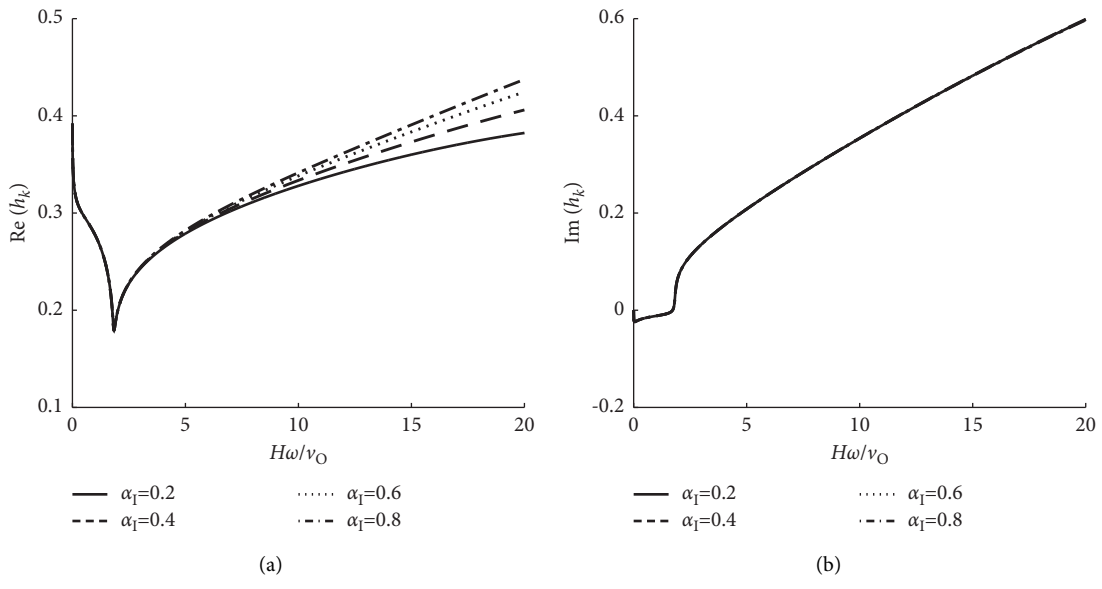


Figure 5: The impedance factor curves of the pile core soil under different fractional derivative orders. (a) Horizontal stiffness factor of the soil layer. (b) Horizontal damping factor of the soil layer.

where $f_{1k} = \alpha_k - (-1)^k \lambda \sinh \lambda/\lambda^2 + \alpha_k^2$, $f_{2k} = (-1)^{k+1}\lambda \cosh \lambda/\lambda^2 + \alpha_k^2$, $f_{3k} = -\alpha_k + (-1)^k \lambda \sin \lambda/\lambda^2 - \alpha_k^2$, and $f_{4k} = (-1)^k \lambda \cos \lambda/\lambda^2 - \alpha_k^2$.

$$U_p(\overline{z}) = \left[\cosh(\lambda\overline{z}) - \sum_{k=1}^{\infty} t_k f_{1k} \sin(\alpha_k \overline{z})\right] C_1 + \left[\sinh(\lambda\overline{z}) - \sum_{k=1}^{\infty} t_k f_{2k} \sin(\alpha_k \overline{z})\right] C_2 + \left[\cos(\lambda\overline{z}) - \sum_{k=1}^{\infty} t_k f_{3k} \sin(\alpha_k \overline{z})\right] C_3 + \left[\sin(\lambda\overline{z}) - \sum_{k=1}^{\infty} t_k f_{4k} \sin(\alpha_k \overline{z})\right] C_4, \tag{35}$$

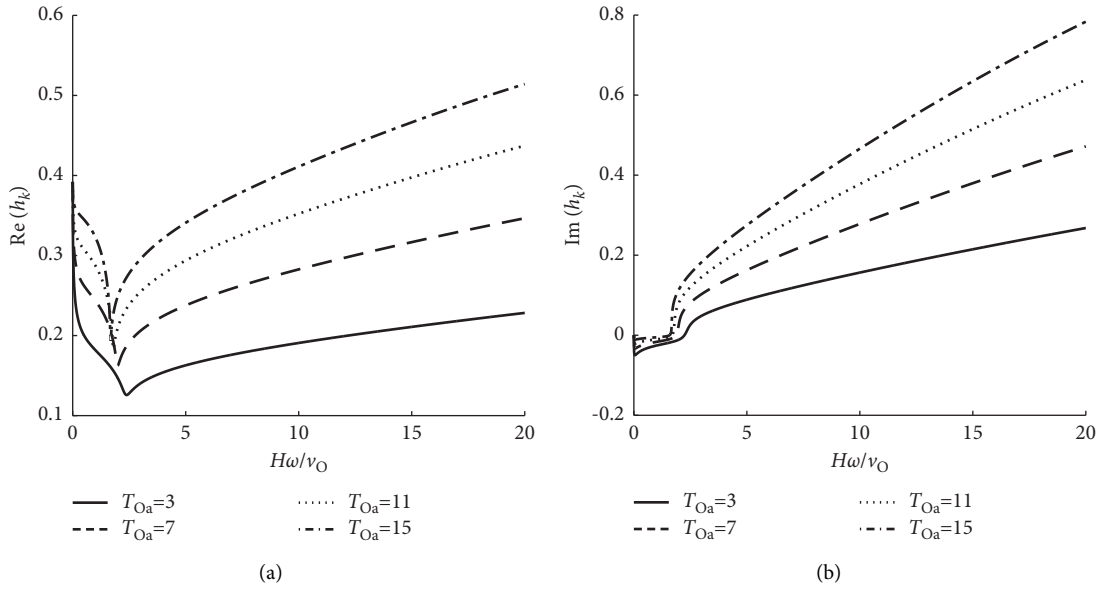


FIGURE 6: The impedance factor curves of soil layers under different model parameters ($T_{Oa}$). (a) Horizontal stiffness factor of the soil layer. (b) Horizontal damping factor of the soil layer.

where $t_k = 8h_k/E(\overline{r}_O^4 - \overline{r}_I^4)(\alpha_k^4 - \lambda^4) + 4h_k$.

For the end-bearing friction pile, since the bottom of the pipe pile is in complete contact with the bedrock, the displacement and rotation angle of the pile bottom are zero, which leads to

$$\begin{bmatrix} 1 & 0 & 1 & 0 \\ -\sum_{k=1}^{\infty} t_k\alpha_k f_{1k} & \lambda - \sum_{k=1}^{\infty} t_k\alpha_k f_{2k} & -\sum_{k=1}^{\infty} t_k\alpha_k f_{3k} & \lambda - \sum_{k=1}^{\infty} t_k\alpha_k f_{4k} \end{bmatrix} \begin{Bmatrix} C_1 \\ C_2 \\ C_3 \\ C_4 \end{Bmatrix} = \begin{Bmatrix} 0 \\ 0 \end{Bmatrix}. \tag{36}$$

When restraining the rotation of pile top, the shear force and bending moment of pipe pile producing a unit horizontal displacement are the horizontal dynamic impedance $K_{hh}$ and the horizontal-swing dynamic impedance $K_{rh}$ of the pipe pile, respectively. When the rotation of pile top is restrained and the horizontal displacement of the pile top is 1, equation (36) can be expressed as

$$\begin{bmatrix} \lambda\sinh\lambda & \lambda\cosh\lambda & -\lambda\sin\lambda & \lambda\cos\lambda \\ \cosh\lambda - \sum_{k=1}^{\infty} t_k f_{1k}(-1)^{k+1} & \sinh\lambda - \sum_{k=1}^{\infty} t_k f_{2k}(-1)^{k+1} & \cos\lambda - \sum_{k=1}^{\infty} t_k f_{3k}(-1)^{k+1} & \sin\lambda - \sum_{k=1}^{\infty} t_k f_{4k}(-1)^{k+1} \end{bmatrix} \begin{Bmatrix} C_1 \\ C_2 \\ C_3 \\ C_4 \end{Bmatrix} = \begin{Bmatrix} 0 \\ 1 \end{Bmatrix}. \tag{37}$$

Combining equations (36) and (37), the coefficients $C_1$, $C_2$, $C_3$, and $C_4$ can be determined. Then, the corresponding shear force and bending moment can be determined, so that the horizontal dynamic impedance $K_{hh}$ can be obtained as

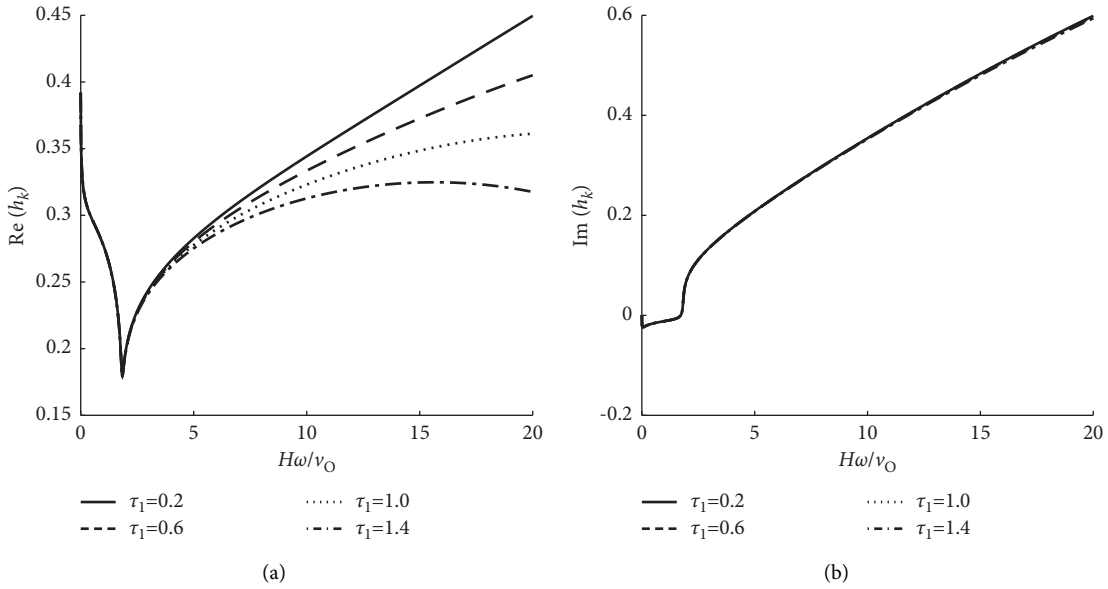


Figure 7: The impedance factor curves of soil layers under different model parameter ratios ($\tau_1 = \tau_{Ia}/\tau_{Oa}$). (a) Horizontal stiffness factor of the soil layer. (b) Horizontal damping factor of the soil layer.

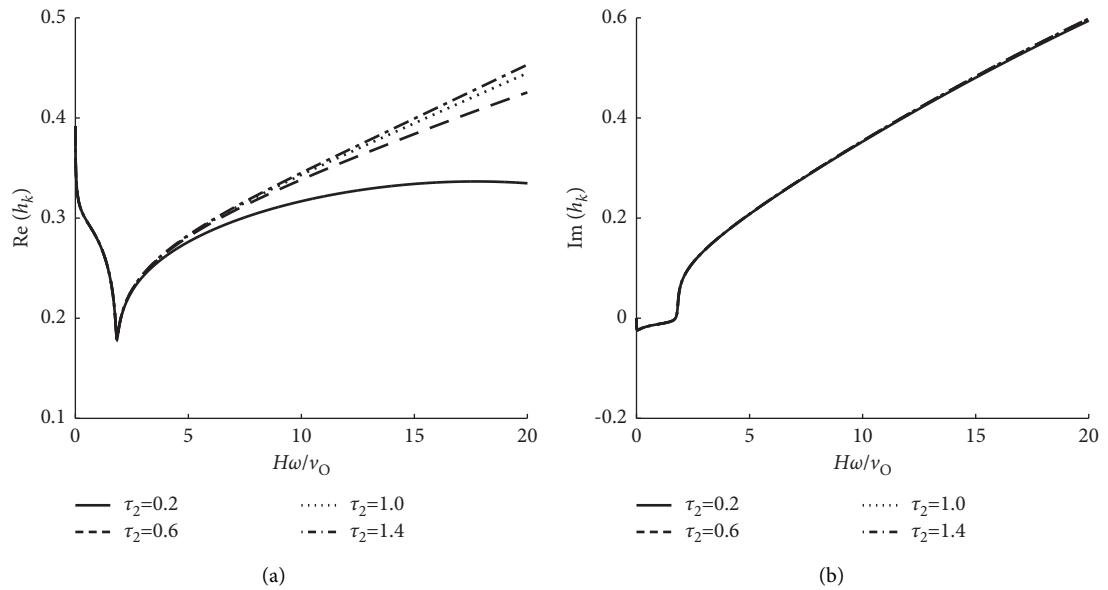


Figure 8: The impedance factor curves of soil layers under different model parameter ratios ($\tau_2 = \tau_{Ib}/\tau_{Ob}$). (a) Horizontal stiffness factor of the soil layer. (b) Horizontal damping factor of the soil layer.

$$K_{hh} = -\frac{\pi E\left(\overline{r}_O^4 - \overline{r}_I^4\right)}{4}\lambda^3\left[C_1\sinh(\lambda) + C_2\cosh(\lambda) + C_3\sin(\lambda) - C_4\cos(\lambda)\right]. \tag{38}$$

In this section, based on fractional derivative viscoelastic model and the soil force of equation (29), the dynamic equations of pipe pile under the horizontal harmonic load are derived. For the pipe pile under the harmonic loads with different frequencies, the variations of the horizontal dynamic impedance, horizontal-swing dynamic impedance, sway dynamic impedance, and horizontal-swing can be analyzed and discussed.

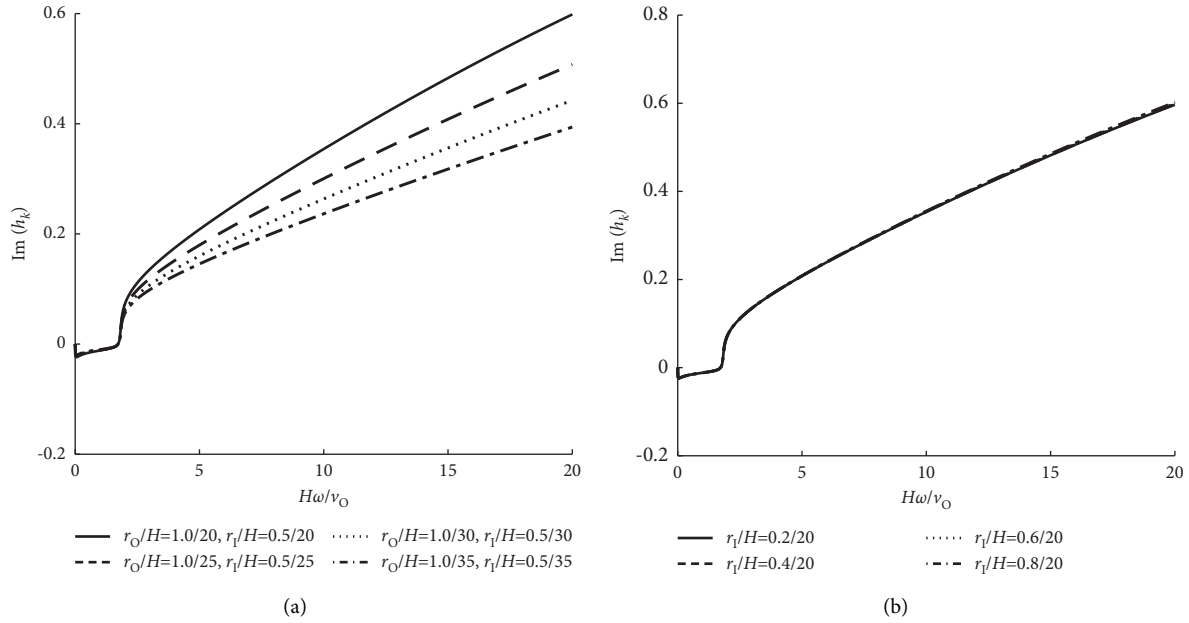


Figure 9: The impedance factor curves of soil layers under different inner radii of pipe pile. (a) Horizontal stiffness factor of the soil layer. (b) Horizontal damping factor of the soil layer.

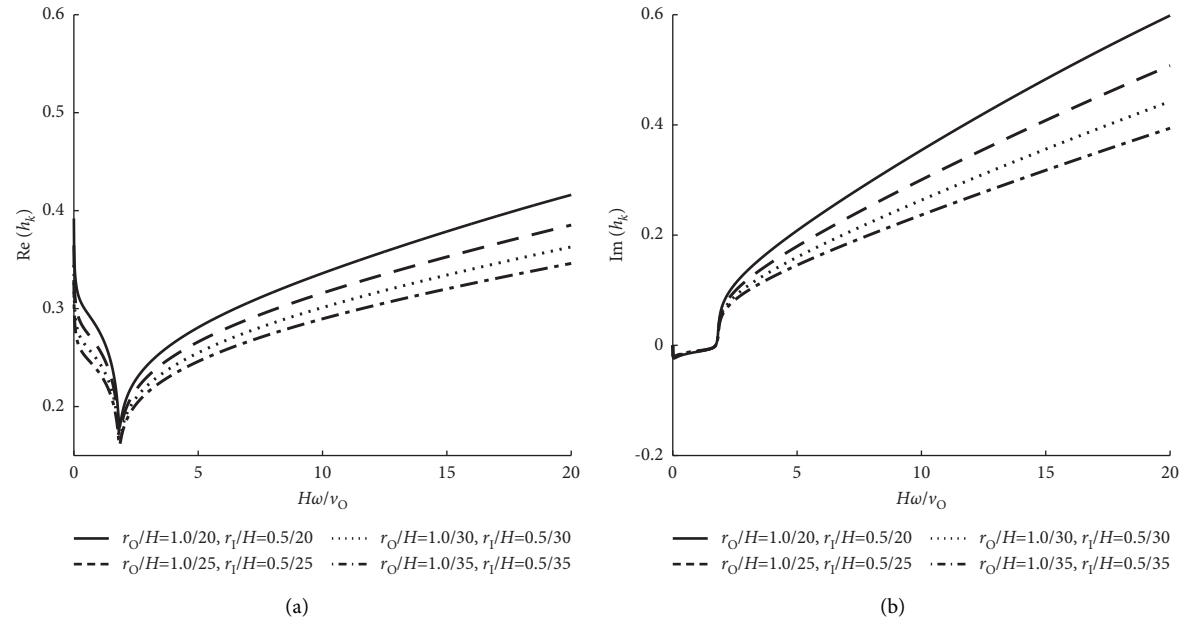


Figure 10: The impedance factor curves of soil layers under different lengths of pipe pile. (a) Horizontal stiffness factor of the soil layer. (b) Horizontal damping factor of the soil layer.

## 6. The Numerical Analysis of Horizontal Impedance Factor of Pipe Pile

In equation (38), the values of the relevant parameters are $r_O/H = 1/20$, $r_I/H = 0.5/20$, $\rho = 1.0$, $G = 0.5$, $\rho_p = 2.0$, $E = 1000$, $\mu_O = 0.3$, $\mu_I = 0.3$, $T_{Oa} = 10$, $T_{Oa} = 20$, $\tau_1 = 0.5$, $\tau_2 = 0.5$, $\alpha_O = 0.5$, and $\alpha_I = 0.5$.The influences of soil model, model parameters, and pipe pile geometry parameters on the horizontal dynamic impedance $K_{hh}$ of pipe pile are analyzed by the numerical solutions.

For the fractional derivative viscoelastic model, classical viscoelastic model, and elastic model of soil layer, the horizontal impedance factor curves of pipe pile are shown in Figure 11. The horizontal dynamic impedance curves of pipe pile by using the fractional derivative viscoelastic model can gradually degenerate to the solutions of the classical viscoelastic and elastic models. Because the elastic model does not consider the effect of damping, the horizontal dynamic impedance in the fractional derivative viscoelastic model is in between the classical viscoelastic model and the elastic model, and the

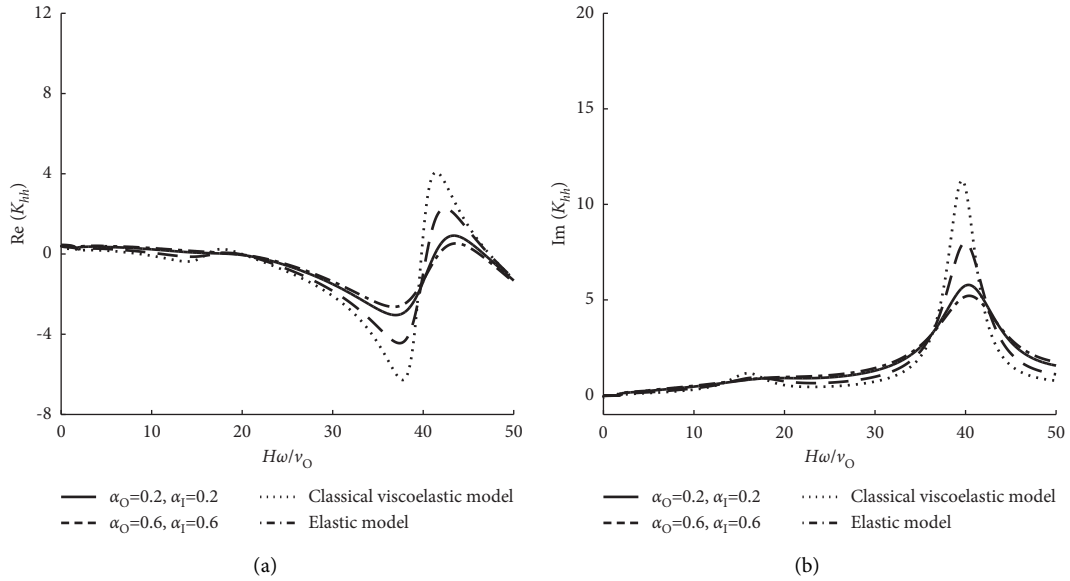


Figure 11: The horizontal dynamic impedance curves of pipe pile under different soil models. (a) Real part of horizontal dynamic impedance. (b) Imaginary part of horizontal dynamic impedance.

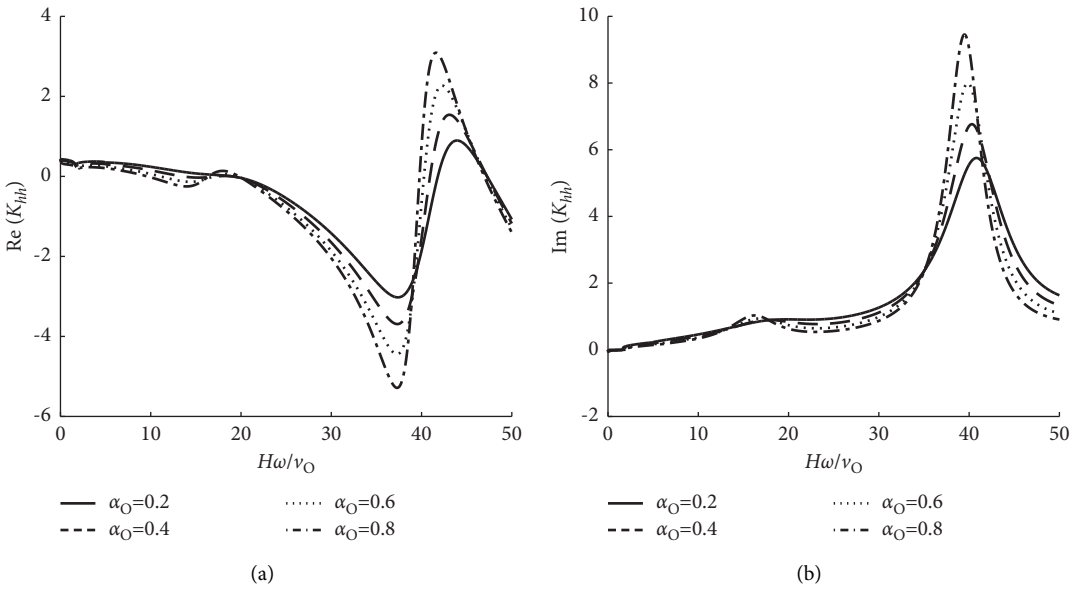


Figure 12: The horizontal dynamic impedance curves of pipe pile under different orders of fractional derivative viscoelastic model of the soil around pile. (a) Real part of horizontal dynamic impedance. (b) Imaginary part of horizontal dynamic impedance.

horizontal dynamic impedance is smaller than that of the classical viscoelastic model and larger than that of the elastic model. It can also be found from Figure 11 that the horizontal dynamic impedance has little difference between the fractional derivative viscoelastic model, classical viscoelastic model, and elastic model when $H\omega/vO < 30$; however, the results of the three models are quite different at high frequency, the variation curves of horizontal dynamic impedance with the frequency variation show obvious fluctuation at high frequency ($H\omega/vO > 30$), and there is a resonance phenomenon in the pipe pile-viscoelastic soil system.

In the fractional derivative viscoelastic model, the influence of the order on the horizontal dynamic impedance of the pipe pile is shown in Figures 12 and 13. For different orders of fractional derivative, the effect of soil around pile on the pile impedance is larger, while the influence of the pile core soil is smaller, which may be due to the fact that the pile core soil has a smaller effect on the pipe pile. As the order of fractional derivative increases, the real and imaginary part peaks of the impedance increase with the increase of the frequency, and the impedance curves fluctuate more obviously.

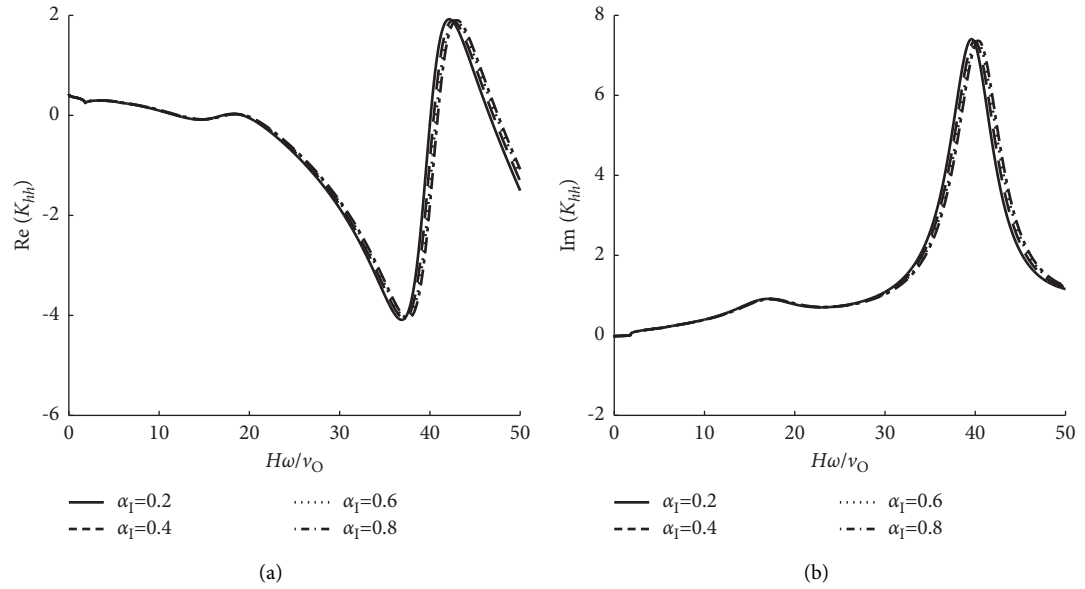


Figure 13: The horizontal dynamic impedance curves of pipe pile under different orders of fractional derivative viscoelastic model of the pile core soil. (a) Real part of horizontal dynamic impedance. (b) Imaginary part of horizontal dynamic impedance.

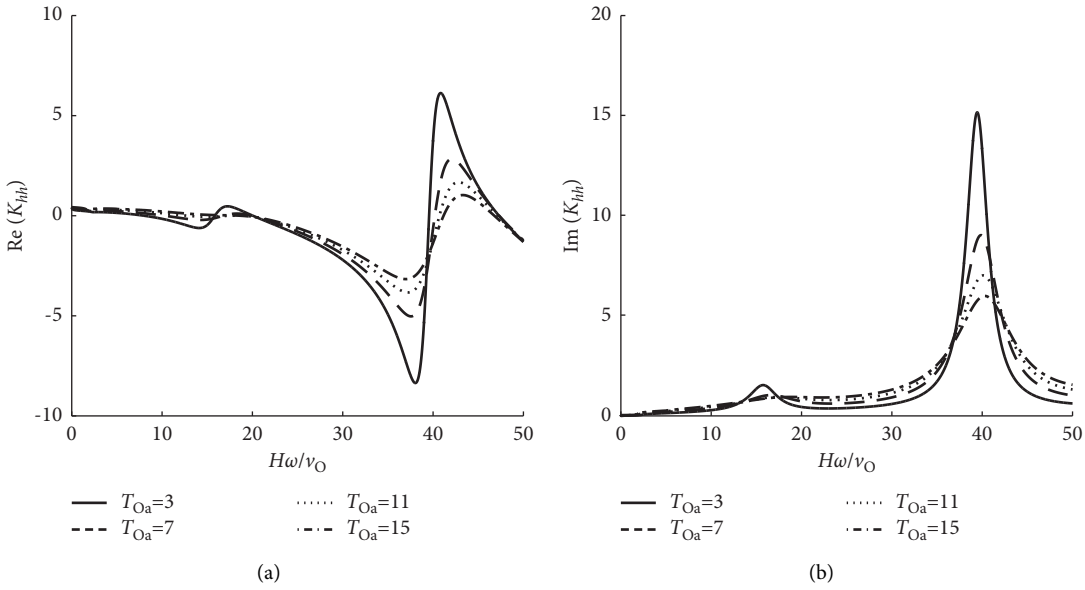


Figure 14: The horizontal dynamic impedance curves of pipe pile under different model parameters ($T_{Oa}$). (a) Real part of horizontal dynamic impedance. (b) Imaginary part of horizontal dynamic impedance.

For the fractional derivative viscoelastic model, the effects of the model parameters on the horizontal dynamic impedance of the pipe pile are shown in Figures 14– 16. The model parameter $T_{Oa}$ of soil around pile has a greater effect on the horizontal dynamic impedance of the pipe pile, while the effects of model parameters $\tau_1 = \tau_{Ia}/\tau_{Oa}$ and $\tau_2 = \tau_{Ib}/\tau_{Ob}$ of pile core soil are smaller. This indicates that the viscosity and elasticity differences of soil around the pile and the pile core soil have little effect on the horizontal dynamic impedance of the pipe pile. As the soil model parameter $T_{Oa}$ is larger, the real and imaginary part peaks of the dynamic impedance curves are smaller, and the fluctuation of the curves is smaller.

The influence of the geometric factor on the horizontal vibration of pipe pile is shown in Figures 17 and 18. The pile core radius and the pile length have a greater influence on the horizontal dynamic impedance of pipe pile. As the pile length is larger, the horizontal dynamic impedance is lower, the fluctuation of real and imaginary part curves shows a gentle trend with the frequency variation, and the influence of pile length on the pile impedance is smaller.

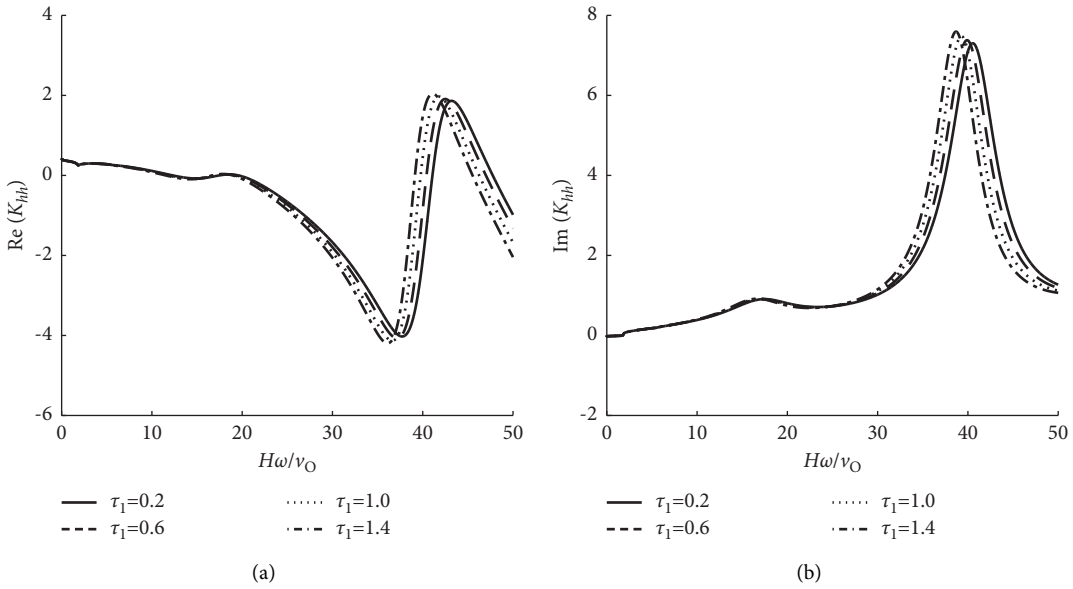


Figure 15: The horizontal dynamic impedance curves of pipe pile under different model parameter ratios ($\tau_1 = \tau_{Ia}/\tau_{Oa}$). (a) Real part of horizontal dynamic impedance. (b) Imaginary part of horizontal dynamic impedance.

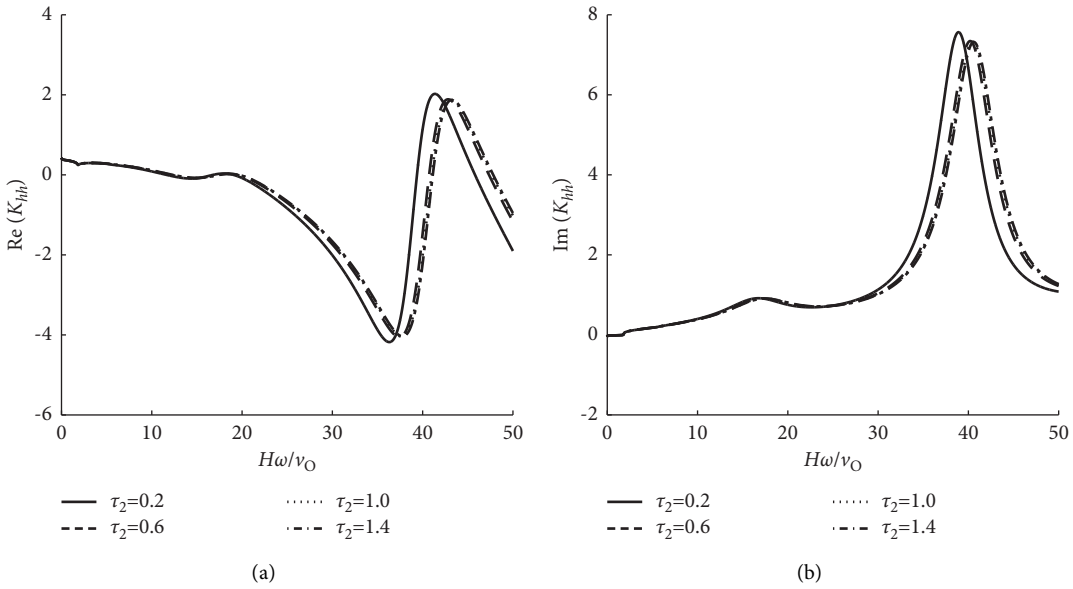


Figure 16: The horizontal dynamic impedance curves of pipe pile under different model parameter ratios ($\tau_2 = \tau_{Ib}/\tau_{Ob}$). (a) Real part of horizontal dynamic impedance. (b) Imaginary part of horizontal dynamic impedance.

In this study, the dynamic equations of pipe-soil system under the horizontal harmonic load are derived by the fractional derivative viscoelastic method. The radial and circumferential displacements of the pile-soil system are solved by the potential function decomposition method, and the forces between soil layers and pipe pile are obtained by the forms of

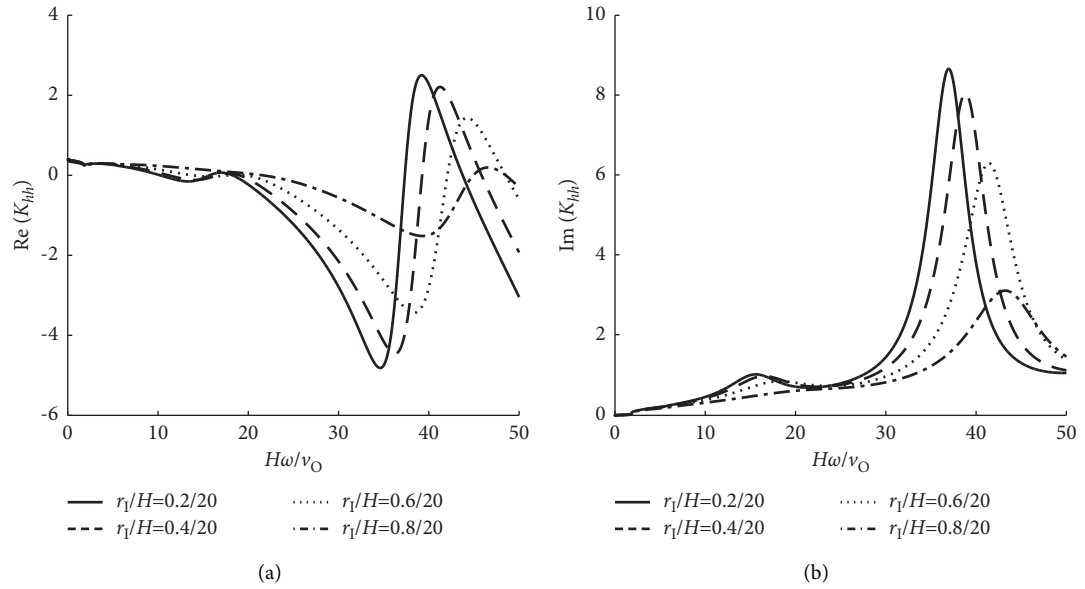


Figure 17: The horizontal dynamic impedance curves of pipe pile with different inner radii. (a) Real part of horizontal dynamic impedance. (b) Imaginary part of horizontal dynamic impedance.

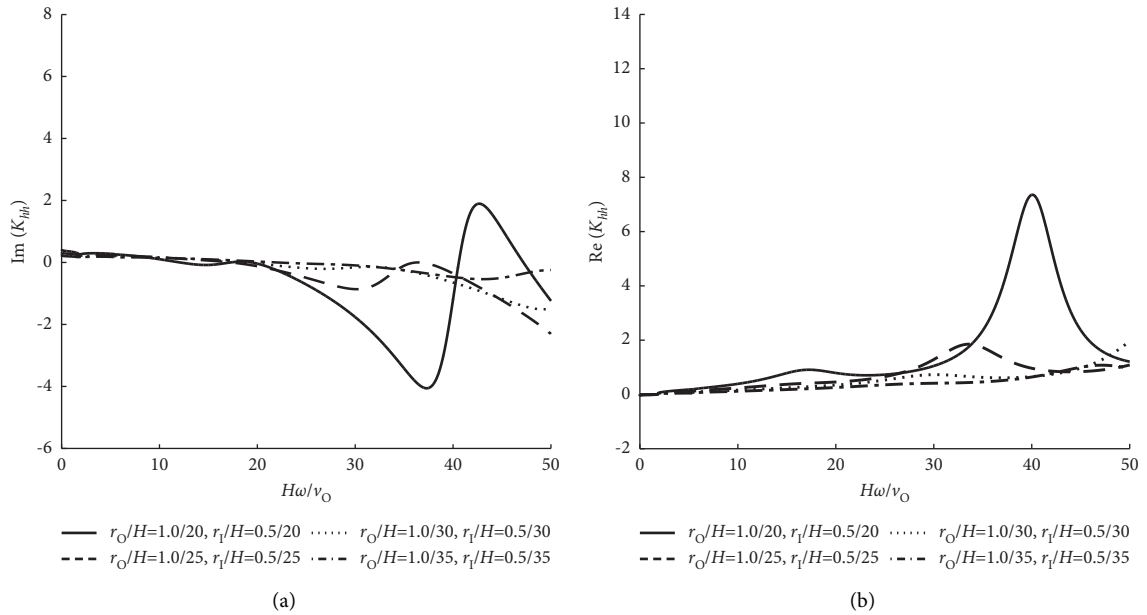


Figure 18: The horizontal dynamic impedance curves of pipe pile under different lengths of pipe pile. (a) Real part of horizontal dynamic impedance. (b) Imaginary part of horizontal dynamic impedance.

series solutions. Furthermore, the numerical solutions are used to analyze the influences of model parameters on the impedance factor of soil layers and the horizontal dynamic impedance of pipe pile. However, the influences of model parameters on the horizontal-swing dynamic impedance, sway dynamic impedance, and horizontal swing of the pipe pile will be investigated in future works.

## 7. Conclusions

In this study, based on the fractional derivative viscoelastic model and three-dimensional wave model, considering the properties of fractional derivative and pipe pile-soil boundary conditions, the impedance factors of soil layer and the horizontal dynamic impedance of pipe pile are obtained

and analyzed by the mathematical-physical means. The following conclusions are obtained:

(1) For the fractional derivative viscoelastic model, classical viscoelastic model, and elastic model of soil layers, the real part curves of the horizontal dynamic impedance has more obvious sharp valleies at the low frequencies, while the real part of the horizontal dynamic impedance is close to a straight line; the impedance factor curves of the soil layer show an obvious fluctuation at the high frequencies, and there exists a resonance phenomenon in the pipe pile-soil system.

(2) By using the fractional derivative viscoelastic model of soil layer, for different orders of the fractional derivative and soil model parameters, the influences of pile around soil on the dynamic impedance are larger than the influences of pile core soil on the dynamic impedance.

(3) As the radius of pile core is larger, the horizontal stiffness factors of soil layers are smaller, and the horizontal dynamic impedance of pipe pile is larger. As the length of pipe pile is larger, the soil horizontal impedance factor is smaller, the horizontal dynamic impedance of pipe pile is smaller, and the influence of pile length on the pile impedance becomes smaller.

## Data Availability

The data used to support the findings of this study are included within the article.

## Conflicts of Interest

The authors declare that they have no conflicts of interest.

## Acknowledgments

This study was supported by the National Natural Science Foundation of China (grant no. U1504505).

## References

[1] J. Lai, S. Mao, J. Qiu et al., "Investigation progresses and applications of fractional derivative model in geotechnical engineering," *Mathematical Problems in Engineering*, vol. 2016, Article ID 9183296, 15 pages, 2016.

[2] K. Yao, Y. S. Liang, and J. X. Fang, "The fractal dimensions of graphs of the Weyl-Marchaud fractional derivative of the Weierstrass-type function," *Chaos, Solitons & Fractals*, vol. 35, no. 1, pp. 106–115, 2008.

[3] M. D. Paola and M. Zingales, "Exact mechanical models of fractional hereditary materials," *Journal of Rheology*, vol. 56, no. 5, pp. 983–1004, 2012.

[4] M. Caputo and M. Fabrizio, "Damage and fatigue described by a fractional derivative model," *Journal of Computational Physics*, vol. 293, no. 15, pp. 400–408, 2015.

[5] W. Chen, S. Hu, and W. Cai, "A causal fractional derivative model for acoustic wave propagation in lossy media," *Archive of Applied Mechanics*, vol. 86, no. 3, pp. 529–539, 2016.

[6] M. Caputo and M. Fabrizio, "On the notion of fractional derivative and applications to the hysteresis phenomena," *Meccanica*, vol. 52, no. 13, pp. 3043–3052, 2017.

[7] T. P. Sales, F. D. Marques, D. A. Pereira, and D. A. Rade, "Dynamic assessment of nonlinear typical section aero-viscoelastic systems using fractional derivative-based visco-elastic model," *Journal of Sound and Vibration*, vol. 423, no. 9, pp. 230–245, 2018.

[8] H.-H. Zhu, L.-C. Liu, H.-F. Pei, and B. Shi, "Settlement analysis of viscoelastic foundation under vertical line load using a fractional Kelvin-Voigt model," *Geomechanics and Engineering*, vol. 4, no. 1, pp. 67–78, 2012.

[9] D. Yin, H. Wu, C. Cheng, and Y. Chen, "Fractional order constitutive model of geomaterials under the condition of triaxial test," *International Journal for Numerical and Analytical Methods in Geomechanics*, vol. 37, no. 8, pp. 961–972, 2013.

[10] D. Li, C. Zhang, G. Ding et al., "Fractional derivative-based creep constitutive model of deep artificial frozen soil," *Cold Regions Science and Technology*, vol. 170, Article ID 102942, 2020.

[11] X.-B. Xu and Z.-D. Cui, "Investigation of a fractional derivative creep model of clay and its numerical implementation," *Computers and Geotechnics*, vol. 119, Article ID 103387, 2020.

[12] M. Novak and F. Aboul-Ella, "Impedance functions of piles in layered media," *Journal of the Engineering Mechanics Division*, vol. 104, no. 3, pp. 643–661, 1978.

[13] T. Nogami and K. Konagai, "Time domain flexural response of dynamically loaded single piles," *Journal of Engineering Mechanics*, vol. 114, no. 9, pp. 1512–1525, 1988.

[14] C. Zheng, G. P. Kouretzis, S. W. Sloan, H. Liu, and X. Ding, "Vertical vibration of an elastic pile embedded in poroelastic soil," *Soil Dynamics and Earthquake Engineering*, vol. 77, no. 5, pp. 177–181, 2015.

[15] W. Wu, H. Liu, M. H. El Naggar, G. Mei, and G. Jiang, "Torsional dynamic response of a pile embedded in layered soil based on the fictitious soil pile model," *Computers and Geotechnics*, vol. 80, no. 3, pp. 190–198, 2016.

[16] Z.-Y. Li and K.-H. Wang, "Vertical dynamic impedance of large-diameter pile considering its transverse inertia effect and construction disturbance effect," *Marine Georesources & Geotechnology*, vol. 35, no. 2, pp. 256–265, 2017.

[17] J. Wang and Y. Gao, "Vertical impedance of a pile in layered saturated viscoelastic half-space considering radial inhomogeneity," *Soil Dynamics and Earthquake Engineering*, vol. 112, no. 1, pp. 107–117, 2018.

[18] J. Wang, D. Zhou, and Y. Zhang, "Vertical impedance of a tapered pile in inhomogeneous saturated soil described by fractional viscoelastic model," *Applied Mathematical Modelling*, vol. 75, pp. 88–100, 2019.

[19] H. Liu, W. Wu, G. Jiang, M. H. El Naggar, G. Mei, and R. Liang, "Influence of soil plug effect on the vertical dynamic response of large diameter pipe piles," *Ocean Engineering*, vol. 157, pp. 13–25, 2018.

[20] C. Cui, K. Meng, Y. Wu, and D. Chapman, "Dynamic response of pipe pile embedded in layered visco elasticmedia with radial inhomogeneity under vertical excitation," *Geomechanics and Engineering*, vol. 16, no. 6, pp. 609–618, 2018.

[21] W. Wu, M. H. El Naggar, and M. Abdlrahem, "New interaction model for vertical dynamic response of pipe piles considering soil plug effect," *Canadian Geotechnical Journal*, vol. 54, no. 7, pp. 987–1001, 2017.

[22] K. Meng, C. Cui, Z. Liang, H. Li, and H. Pei, "A new approach for longitudinal vibration of a large-diameter floating pipe pile in visco-elastic soil considering the three-dimensional wave effects," *Computers and Geotechnics*, vol. 128, Article ID 103840, 2020.

[23] R. L. Bagley and P. J. Torvik, "A theoretical basis for the application of fractional calculus to viscoelasticity," *Journal of Rheology*, vol. 27, no. 3, pp. 201–210, 1983.

[24] K. S. Miller and B. Ross, *An Introduction to the Fractional Calculus and Fractional Differential Equations*, Wiley, Hoboken, NJ, USA, 1993.

[25] T. Nogami and M. Novak, "Resistance of soil to a horizontally vibrating pile," *Earthquake Engineering & Structural Dynamics*, vol. 5, no. 3, pp. 249–261, 1977.